

# A Defined Locus Control Region Determinant Links Chromatin Domain Acetylation with Long-Range Gene Activation

Yugong Ho, Felice Elefant, Nancy Cooke, and Stephen Liebhaber<sup>1</sup>

Departments of Genetics and Medicine  
University of Pennsylvania  
Philadelphia, Pennsylvania 19104

## Summary

Gene activation in higher eukaryotes is often under the control of regulatory elements quite distant from their target promoters. It is unclear how such long-range control is mediated. Here we show that a single determinant of the human growth hormone locus control region (*hGH* LCR) located 14.5 kb 5' to the *hGH-N* promoter has a critical, specific, and nonredundant role in facilitating promoter *trans* factor binding and activating *hGH-N* transcription. Significantly, this same determinant plays an essential role in establishing a 32 kb acetylated domain that encompasses the entire *hGH* LCR and the contiguous *hGH-N* promoter. These data support a model for long-range gene activation via LCR-mediated targeting and extensive spreading of core histone acetylation.

## Introduction

Eukaryotic gene activation is dependent on chromatin modifications that facilitate access of *trans* factors to cognate DNA binding sites (Felsenfeld et al., 1996). Core histone acetylation, the best described of these modifications, is positively correlated with transcriptional activation (Grunstein, 1997; Kuo and Allis, 1998; Struhl, 1998). Although histone acetylation is most commonly targeted to nucleosomes in the immediate locale of promoters and their proximal enhancer determinants, it can also be involved in the establishment of extensive "activated" chromatin domains (Hebbes et al., 1994; Schubeler et al., 2000; Elefant et al., 2000a). How these domains are established and how they function in gene control are questions of significant interest.

Locus control regions (LCRs) are operationally defined by their ability to activate the robust expression of linked transgenes in a tissue-specific and copy number-dependent manner irrespective of where they insert in the host genome (Grosveld et al., 1987; Festenstein et al., 1996). LCRs have been described in a broad spectrum of mammalian gene systems, suggesting that they play a substantial role in the overall control of eukaryotic gene expression (reviewed in Li et al., 1999). The components of an LCR commonly colocalize to sites of DNaseI hypersensitivity (HS) in the chromatin of expressing cells. In the limited number of LCR determinants studied in detail, the core determinants at individual HS are composed of arrays of multiple transcription factor binding sites (Li et al., 1999). It remains unclear how the corresponding *cis/trans* interactions mediate LCR function

and how they specifically mediate long-range gene activation.

The human *growth hormone* (*hGH*) gene cluster constitutes a highly informative model of developmentally controlled gene expression. This cluster encompasses *hGH-N*, expressed primarily in pituitary somatotropes and four genes, *hCS-A*, *hCS-B*, *hCS-L*, and *hGH-V*, expressed specifically in syncytiotrophoblast cells lining the placental villi (Chen et al., 1989; Cooke and Liebhaber, 1995) (Figure 1A). A multicomponent LCR is required for transcriptional activation in both expressing tissues (Jones et al., 1995; Su et al., 2000). This LCR contains five DNaseI hypersensitive sites (HS) distributed in the region between 14.5 kb and 32 kb 5' to the cluster. HSI and HSII, located –14.5 kb and –15.3 kb with respect to the *hGH-N* promoter, are specific to pituitary chromatin (Figure 1A). A 1.6 kb genomic fragment encompassing HSI and HSII is sufficient to activate high-level expression of a directly linked *hGH-N* transgene and its minimal promoter in somatotrope cells in vivo (Jones et al., 1995). The activity of this HSI,II region has been sublocalized to its extreme 3' terminus by transgenic mapping studies (Bennani-Baiti et al., 1998a; Shewchuk et al., 1999). This active site, centered at –14.5 kb relative to the *hGH-N* promoter, corresponds to the position of HSI as determined by high-resolution mapping of primary pituitary chromatin (Jones et al., 1995). An array of three Pit-1 binding sites has been identified within this HSI subregion (Figure 1A); interruption or deletion of two of these three Pit-1 binding sites results in loss of gene activation when assessed in a transgene reporter assay (Shewchuk et al., 1999). A central question that follows from these findings is whether the HSI determinants play a unique, nonredundant role in activation of the *hGH-N* gene when separated from the target *hGH-N* promoter by 14.5 kb and how such long-range gene activation is accomplished.

The function of the *hGH* LCR has been linked to specific patterns of core histone acetylation. In the pituitary, the LCR is encompassed in a somatotrope-specific domain of hyperacetylated chromatin that extends from the most 5' LCR component (HSV; –32 kb) to the *hGH-N* promoter (Elefant et al., 2000a). This domain of chromatin modification was initially observed in primary human somatotrope adenomas and is faithfully recapitulated in the pituitaries of transgenic mice carrying the *hGH* LCR and contiguous *hGH* gene cluster (Elefant et al., 2000a). The pituitary-specific HSI and HSII are situated at the central and most highly modified region of this domain. The tissue specificity and pattern of acetylation in this region, along with the functional mapping studies, suggest that determinants coincident with HSI may play a unique role in *hGH-N* activation via targeting and subsequent spreading of HAT coactivator function (Elefant et al., 2000a).

The present study directly tests the central role of HSI in LCR-mediated chromatin modification and in the activation of the remote *hGH-N* gene promoter. A 99 bp subfragment containing two of the previously identified Pit-1 sites critical to the activity of the isolated HSI

<sup>1</sup>Correspondence: liebhab@mail.med.upenn.edu

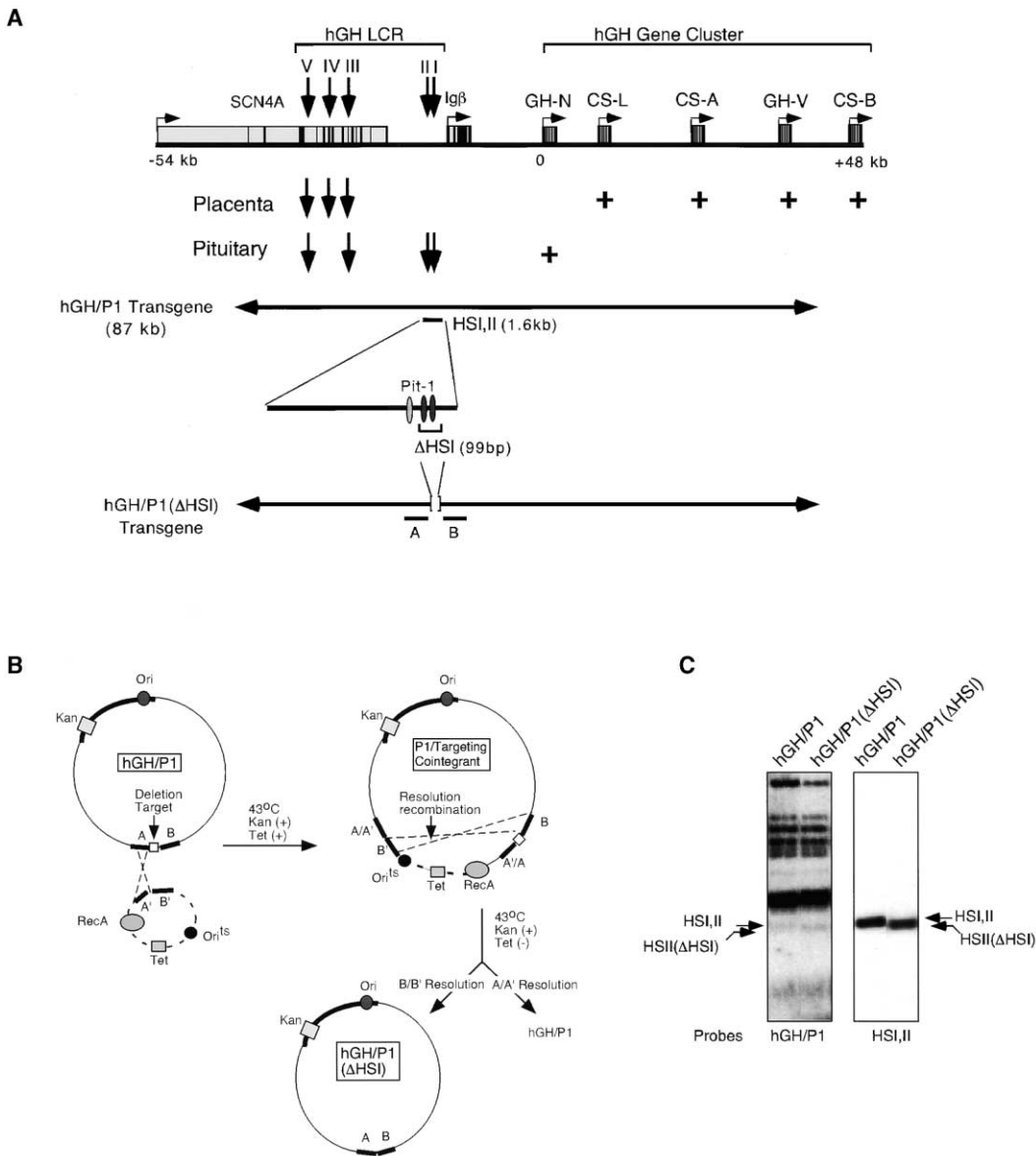


Figure 1. Physical Map of the *hGH* Cluster and Targeted Deletion of HSI

(A) Diagram of the *hGH* locus and corresponding P1 transgenes. The position and tissue specificity of each DNaseI HS are indicated (downward arrows). The five genes of the *hGH* cluster are shown; each comprises five exons (dark vertical lines) and all are in the same transcriptional orientation. Two genes that overlap with the *hGH* LCR determinants are the B lymphocyte-specific *Igβ* (Bennani-Baiti et al., 1998b) and striated muscle-specific *SCN4A* (Bennani-Baiti et al., 1995). The extent of the 87 kb *hGH/P1* transgene is shown (double-headed arrow), and the previously characterized 1.6 kb *Bgl*III fragment containing the pituitary-specific HSI,II region (Jones et al., 1995) is indicated (underline). An expanded view of the HSI,II region shows the positions of three Pit-1 binding sites that colocalize with HSI (Shewchuk et al., 1999). The last line represents the *hGH/P1(ΔHSI)* transgene that was generated by deletion of a 99 bp fragment encompassing the two adjacent 3' Pit-1 binding sites.

(B) Strategy to generate the 99 bp targeted deletion. Two homology arms that flank the targeted deletion site were generated by PCR and directly fused in their native orientations (recombination arms A and B, respectively). This fragment was subcloned into a special shuttle vector that was cotransfected along with *hGH/P1* into *E. coli*. Cointegrants formed via homologous recombination at either homology arm A or B (the former is shown in the diagram). Resolved cointegrants were selected (see Experimental Procedures).

(C) Structural confirmation of the 99 bp deletion in *hGH/P1*. *hGH/P1* and modified *hGH/P1* DNA were doubly digested with *Eco*RI and *Bgl* II and analyzed by Southern blotting using a labeled *hGH/P1* probe (left panel) or an HSI,II probe (right panel). The left panel shows that *hGH/P1* with the 99 bp deletion [*hGH/P1(ΔHSI)*] and the original *hGH/P1* have identical "fingerprints" with the exception of the faint band encompassing the targeted 99 bp deletion. The right panel selectively identifies the deletion fragment.

(Shewchuk et al., 1999) were selectively deleted from *hGH/P1*, an 87 kb human genomic transgene (Figure 1A). The *hGH/P1* transgene encompasses the entire

*hGH* LCR and the majority of the linked *hGH* gene cluster. This transgene has been previously characterized in detail and has been shown to faithfully recapitulate

pituitary and placental patterns of gene expression from the *hGH* gene cluster (Su et al., 2000). The site-specific deletion has a major impact on the local chromatin structure at HSI, on chromatin modification throughout the *hGH* LCR, on promoter occupancy by a critical *trans* factor, and on activation of *hGH-N* gene expression. These data support a model in which long-range activation of the *hGH-N* gene promoter by HSI is mediated by site-specific recruitment and subsequent spreading of HAT coactivator activity over this large domain.

## Results

### Deletion of Two Pit-1 Binding Sites at HSI of the *hGH* LCR

To investigate the function of HSI within its native context, two of its functional Pit-1 binding sites (Shewchuk et al., 1999) were deleted from an 87 kb human genomic transgene encompassing the entire *hGH* LCR and much of the contiguous *hGH* gene cluster (*hGH/P1*; Figure 1A). Prior studies had demonstrated that the *hGH/P1* transgene constitutes a reliable model of *hGH* LCR function. It encompasses all determinants necessary to direct tissue-specific, copy number-dependent, and site-of-integration-independent control of the various genes in the *hGH* cluster (Su et al., 2000), and it accurately recapitulates site-specific chromatin modifications in human pituitary tissue (Elefant et al., 2000a). Several systems for introducing targeted modification in a large genomic clone have been reported (Shashikant et al., 1998 and references therein; Zhang et al., 1998). In the present case, a 99 bp deletion encompassing the two targeted Pit-1 binding sites was created by RecA-assisted homologous recombination in *E. coli* (Yang et al., 1997) (Figure 1B). The desired deletion was first established in a targeting vector encoding RecA and tetracycline (Tet) resistance, and containing a temperature-sensitive origin of replication (*pSV1.RecA*) (O'Connor et al., 1989; Hamilton et al., 1989). This shuttle vector, which cannot replicate at temperatures above 42°C, was cotransformed into a *recA*<sup>-</sup> *E. coli* strain transformed along with the target *hGH/P1* plasmid carrying a kanamycin (Kan) resistance gene. Cointegrants formed by recombination between one of the "arms" (A or B; arm A in Figure 1B) were selected by dual antibiotic resistance (Tet and Kan) at 43°C, and the recombination event was confirmed by targeted PCR. A subset of the cointegrant plasmids undergoes a second (resolution) recombination event through either arm A or B (arm B in Figure 1B). The resolved P1 plasmids were selected on the basis of antibiotic sensitivity and growth at 43°C. Clones containing the deletion were identified by colony hybridization, and their structures were confirmed by DNA sequencing. The overall structure of the deletion *hGH/P1* plasmid was confirmed by a "fingerprinting" assay; aside from the intentional 99 bp deletion, no other rearrangements, deletions, or insertions in the derivative clone were observed (Figure 1C).

The deleted *hGH/P1* clone was linearized within vector sequences and was microinjected into fertilized mouse oocytes. Six independent transgenic mouse lines carrying the mutated *hGH* LCR were generated. The integrity of the transgenes was determined by Southern

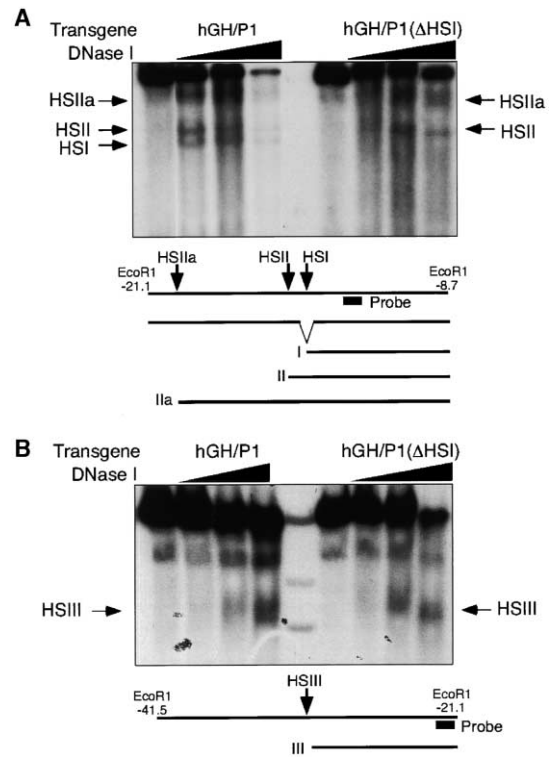


**Figure 2. Selective Inactivation of HSI by the Targeted Deletion**  
Nuclei were isolated from pituitaries of doubly transgenic mice generated from crosses of the *hGH/P1* or *hGH/P1(ΔHSI)* transgenic lines with an *hGRF* transgenic line (see text). The pituitary nuclei were digested with DNaseI for increasing periods of time, digested with *EcoRI*, and then analyzed by Southern blotting using the [<sup>32</sup>P]-labeled probes indicated.  
(A) DNaseI mapping of *hGH/P1* with and without the 99 bp deletion. The bands on the autoradiograph corresponding to HSI and HSIa are indicated; HSI is specifically absent in the *hGH/P1* deletion line [*hGH/P1(ΔHSI)* lanes]. HSIa is a minor, pituitary-specific HS (Jones et al., 1995).  
(B) Detection of HSIII. The band on the autoradiograph corresponding to HSIII is indicated, and the schematic of the indirect end-labeling approach is shown below the gel.

blot of F1 tail DNA from each line (data not shown). The transgene copy numbers were determined by Southern analysis. Founders were crossed with CD1 mates to generate F1 transgenic mice that were used for all subsequent studies.

### Pit-1 Binding Sites Constitute Core Components of HSI

The impact of deleting the two Pit-1 binding sites at HSI was first assessed at the level of chromatin structure (Figure 2). DNaseI mapping was performed on nuclei isolated from the pituitaries of *hGH/P1* mice and mice carrying the *hGH/P1* with the Pit-1 binding site deletion. In this experiment and in those that follow, the somatotrope population was selectively expanded to facilitate chromatin analysis by crossing each transgenic line with a line carrying a human growth hormone releasing factor (*hGRF*) transgene (Mayo et al., 1988). The pituitaries of the doubly transgenic mice were five to ten times normal size due to hGRF-mediated somatotrope hyperplasia.

Pituitaries from five individual *hGH/P1* × *hGRF* mice were pooled for the analysis of each line. Consistent with our prior studies, HSI and HSI<sub>II</sub> were both detected in pituitary chromatin of *hGH/P1* transgenic mice (Jones et al., 1995) (Figure 2A). In contrast, deletion of the two Pit-1 sites at HSI resulted in selective loss of HSI from pituitary chromatin; formation of the remaining HS of the *hGH* LCR (HS<sub>II</sub> and HS<sub>III</sub>) were retained (Figures 2A and 2B). HSV could not be visualized in this study because of the presence of a comigrating mouse endogenous fragment (Jones et al., 1995). These data suggested that the two Pit-1 binding sites, located 14.5 kb upstream to the *hGH-N* promoter, constitute essential core components of HSI within the *hGH* LCR. Based on these data, the mutated *hGH/P1* transgene is referred to as *hGH/P1(ΔHSI)*.

#### Inactivation of HSI Resulted in a Marked Loss of Core Histone Acetylation throughout the *hGH* LCR and at the Contiguous *hGH-N* Promoter

The role of HSI in core histone acetylation at the *hGH* locus was next determined. Pituitary chromatin samples from three independent *hGH/P1(ΔHSI)* lines (946C, 960G, and 961E) were analyzed by chromatin immunoprecipitation (ChIP) using antibodies specific to acetylated forms of histones H3 and H4. Pituitary chromatin samples from two representative mouse lines carrying an intact *hGH/P1* transgene (809F and 811D) (Su et al., 2000) were also assayed. The level of core histone acetylation at each site within the *hGH* LCR was quantified by slot-blot hybridization. Each transgene locus was scanned from a position 6 kb 5' to HSV (−38 kb relative to the *hGH-N* gene), through the entire LCR, and into the *hGH* gene cluster using a series of 15 unique sequence DNA hybridization probes (Figure 3A). To control for DNA loading on the hybridization membrane, the ratio of bound (immunoprecipitated) to unbound DNA at each site was normalized to the corresponding ratio detected by rehybridizing the membrane with a mouse total genomic DNA probe; this total genomic acetylation ratio (bound:unbound) was defined as 1.0. Each of the normalized ratios was plotted as a function of its position along the locus (Figures 3A and 3B). In agreement with prior studies (Elefant et al., 2000a), the pituitary chromatin from the two *hGH/P1* lines contained a 32 kb acetylated domain. This chromatin domain peaked centrally at a site coincident with pituitary-specific HSI<sub>II</sub> and extended in a tapering fashion for approximately 16 kb in both 5' and 3' directions (Figure 3A). The level of *hGH-N* promoter acetylation at the 3' terminus of this domain was approximately 3.5-fold over total genomic background levels; the acetylation of HSV at the 5' border of the domain was at similar levels. The histone acetylation patterns in these two *hGH/P1* lines were essentially identical (Figure 3A) and faithfully recapitulated the pattern observed previously in primary human somatotropes (Elefant et al., 2000a). The consistency of these data indicated that the pattern of acetylation observed in the *hGH/P1* transgene was established in a site-of-integration-independent manner.

The role of HSI in establishing the acetylated domain at the *hGH* locus was next assessed by ChIP analysis of representative deletion lines. These studies revealed

that deletion of core Pit-1 binding sites at HSI resulted in a generalized loss of acetylation throughout the *hGH* LCR and at the contiguous *hGH-N* promoter (Figure 3B). This loss was observed in all three *hGH/P1(ΔHSI)* lines examined. The level of acetylation at the center of the domain decreased from approximately 9-fold over genomic background in the wild-type *hGH/P1* transgene to levels barely above background (ratios of 1.0–2.3) in the *hGH/P1(ΔHSI)* lines. The loss of acetylation extended across the LCR domain to both sides of the central peak. The levels of acetylation at the *hGH-N* promoter in the *hGH/P1* lines decreased from 3.5- and 3.8-fold over genomic background to levels that were indistinguishable from background in the *hGH/P1(ΔHSI)* lines (ratios of 0.7–1.3). A possible exception to the global loss of histone acetylation in the *hGH/P1(ΔHSI)* lines was noted at HSV (−32 kb). The acetylation levels at HSV observed in the two wild-type *hGH/P1* transgenes (ratios of 3.0 and 4.0) were maintained in two of the three *hGH/P1(ΔHSI)* lines (ratios of 3.3 and 2.4) (Figures 3A and 3B). Of note, levels of core histone acetylation outside the domain, i.e., 5' of HSV (p7 and p8) and 3' of the *hGH-N* promoter (p9 and p10), overlapped in the *hGH/P1* and *hGH/P1(ΔHSI)* lines (Figures 3A and 3B). These data indicated that an extensive domain of acetylated chromatin 5' to the *hGH* gene is uniquely dependent on HSI function.

The above studies (Figure 3) were carried out using pooled antibodies to acetylated histones H3 and H4. To confirm and extend these data, pituitary chromatin samples from the two *hGH/P1* lines were reanalyzed by ChIP using the individual antibodies against acetylated H3 and acetylated H4. The individual patterns of H3 (Figure 4A) and H4 (Figure 4B) acetylation across the locus were both in general agreement with the data obtained using the combined antibodies. The levels of acetylation were above baseline throughout the domain and peaked centrally at HSI<sub>II</sub> in both cases. Differences between the patterns of H3 and H4 acetylation were also noted. H3 acetylation appeared to be most prominent 5' to HSI, with lower levels in the region between HSI and the *hGH-N* promoter. In contrast, the pattern of H4 modifications was fairly symmetrical. The selective drop in H3 modification 3' to HSI may underlie the asymmetry of the combined H3 and H4 acetylation curve, which drops more steeply in this region compared with the more gradual taper 5' to the central peak (Figure 3A).

ChIP analysis with the individual antibodies to acetylated H3 and H4 was next carried out on a representative *hGH/P1(ΔHSI)* line. Deletion of HSI resulted in a generalized loss of both H3 and H4 acetylation throughout the *hGH* locus (Figures 4A and 4B). These data were in full agreement with the acetylation patterns observed in the three *hGH/P1(ΔHSI)* lines using the mixed antisera (Figure 3B). Of additional note, the levels of both H3 and H4 acetylation at the *hGH* promoter were reduced to background genomic levels (ratios of 1.0 and 1.1, respectively). Interestingly, low residual levels of acetylation of H4 (approximately 2-fold over background), but not H3, were maintained from HSI<sub>II</sub> through HSV in the *hGH/P1(ΔHSI)* lines. The levels of histone H3 and H4 acetylation outside of the HSI-dependent domain were unaffected by the presence or absence of HSI function (p7 and p10 in Figures 4A and 4B).

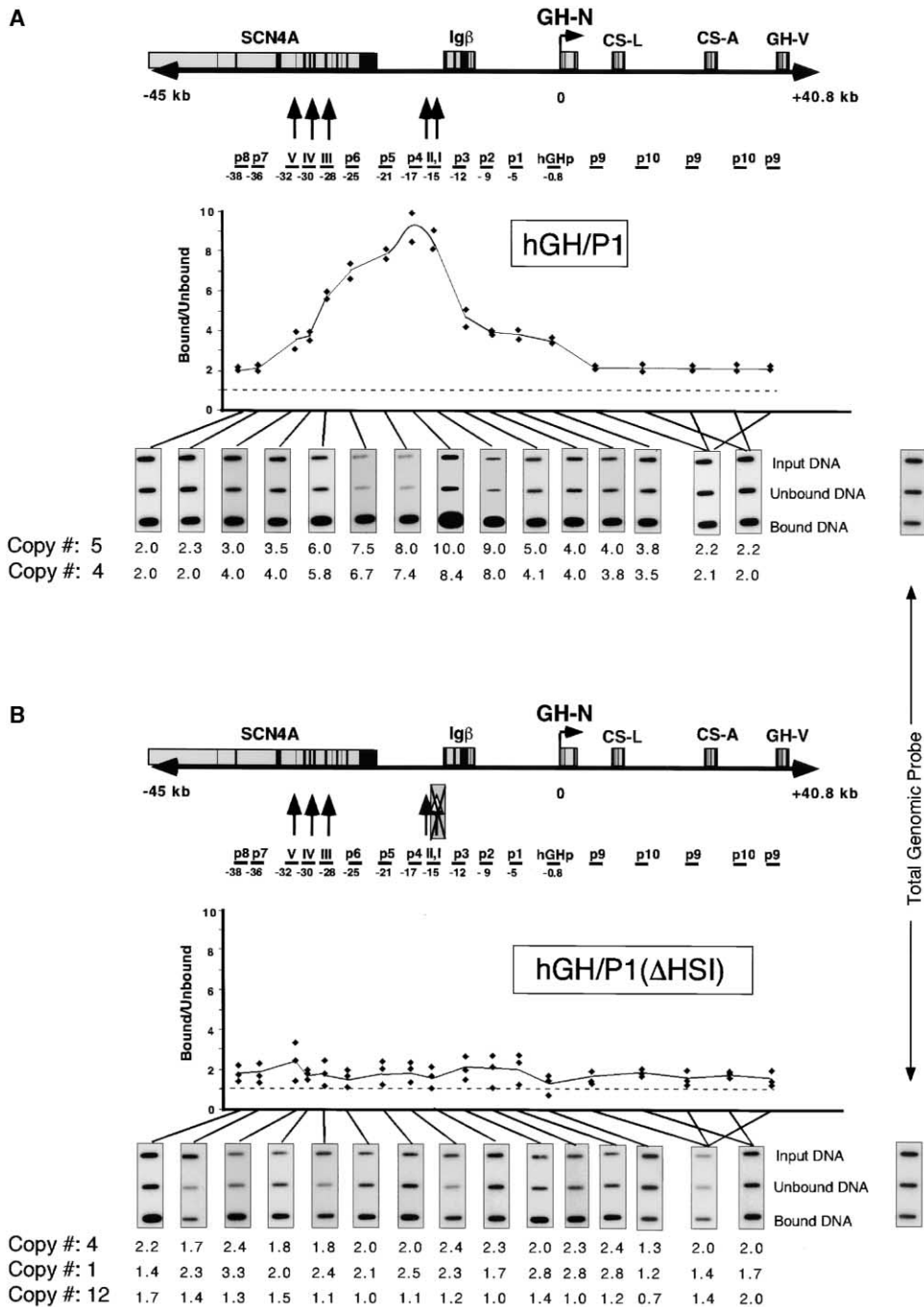
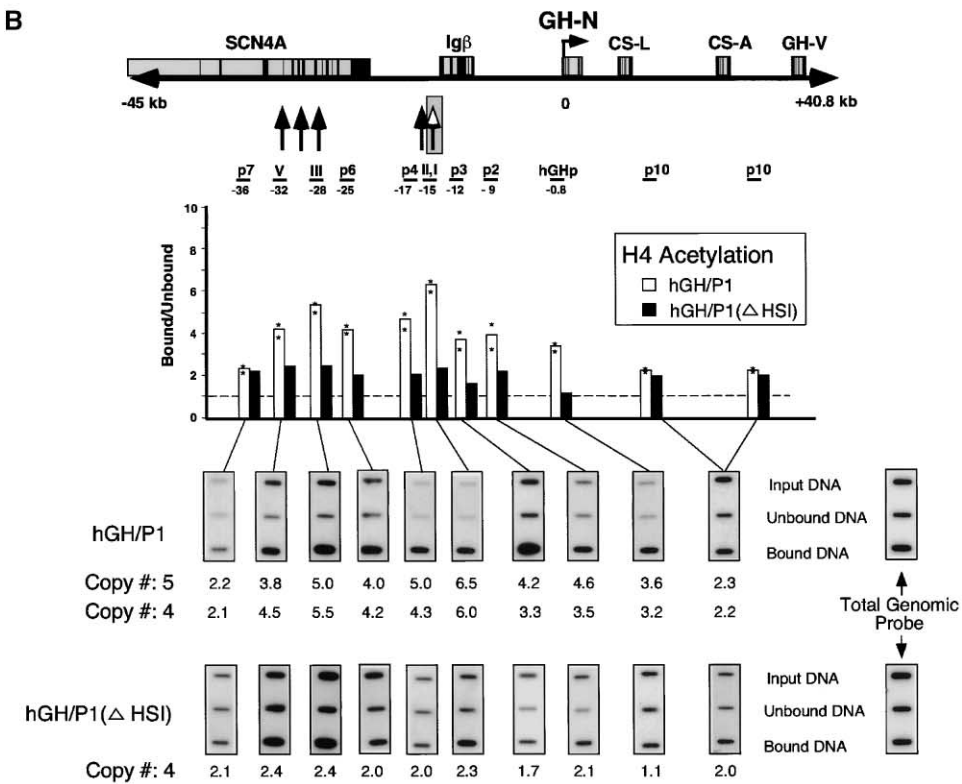
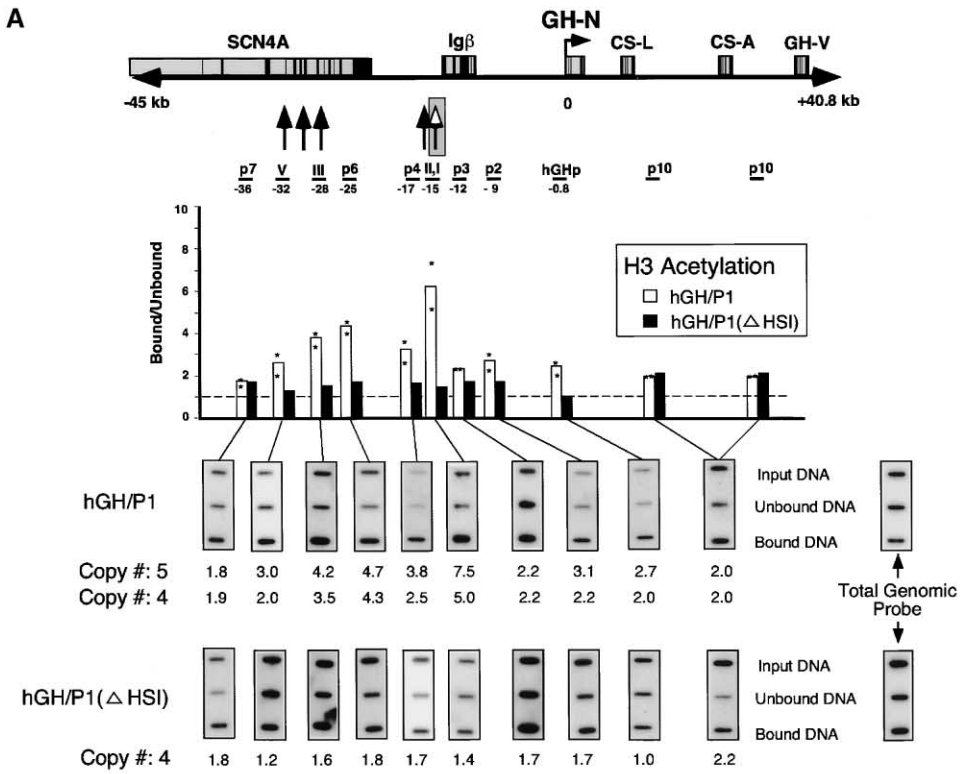


Figure 3. Deletion of HSI Resulted in Global Loss of Histone Acetylation within the *hGH* LCR and at the Remote *hGH-N* Promoter

(A) Acetylation status of chromatin encompassing the *hGH* LCR and *hGH* gene cluster in *hGH/P1* transgenic mouse pituitaries. The map is as described in Figure 1. Positions of the hybridization probes are underlined; the central coordinate of each probe is noted in relation to the transcription initiation site of *hGH-N* (0). The *hGH/P1* lines used in the assays contained five or four tandem copies of the transgenes (lines 809F and 811D). Soluble chromatin samples from 10 to 15 pituitaries of *hGH/P1* × *hGRF* doubly transgenic mice were immunoprecipitated with a mixture of antibodies against acetylated H3 and H4. A representative set of slot-blot autoradiograph (line 809F) corresponding to each of the [<sup>32</sup>P]-probes is shown below the corresponding bar of the histogram. The membrane was reprobbed with [<sup>32</sup>P]-labeled total genomic mouse DNA as control (shown at far right). The ratios of bound (immunoprecipitated) to unbound hybridization signals were determined, normalized to mouse total genomic DNA, and plotted. The acetylation of total genomic DNA was defined as 1.0 (dashed line).

(B) Acetylation status of chromatin encompassing the *hGH* LCR and *hGH* gene cluster in *hGH/P1(ΔHSI)* transgenic mouse pituitaries. HSI is highlighted (shaded box with X) to indicate its deletion in the *hGH/P1(ΔHSI)* transgene. A ChIP assay identical to that described in (A) was carried out on three *hGH/P1(ΔHSI)* transgenic mouse lines (946C, 960G, and 961E). The representative series of autoradiographs shown are from the 960G line.



Thus, comparison of histone acetylation patterns at the *hGH* locus in pituitary chromatin of *hGH/P1* and *hGH/P1(ΔHSI)* transgenic mice demonstrated that the extensive domain of core histone acetylation throughout the *hGH* LCR and at the contiguous *hGH-N* promoter was dependent upon the function of HSI. Analyses of individual H3 and H4 acetylation patterns indicated that both contributed to the overall pattern of chromatin modification, although potentially informative distinctions may exist in their respective contributions and underlying mechanisms.

#### Inactivation of HSI Resulted in Marked Reduction of *hGH-N* Transgene Expression

The impact of HSI inactivation on the expression of the *hGH-N* locus was assessed. Levels of *hGH-N* mRNA were quantified in the pituitaries of each of six separate *hGH/P1(ΔHSI)* transgenic lines (Figure 5A). *hGH-N* transgene expression was measured relative to endogenous *mGH* mRNA by a previously validated coRT-PCR assay (Jones et al., 1995), and the resultant expression levels were normalized to transgene copy number. The corresponding normalized levels of *hGH-N* mRNA from a series of *hGH/P1* lines (Su et al., 2000) were analyzed in parallel. Consistent with prior studies (Jones et al., 1995; Su et al., 2000), *hGH-N* expression from the intact *hGH/P1* transgene was robust and copy number dependent. Expression per transgene copy was 35%–55% of endogenous *mGH* mRNA. Inactivation of HSI resulted in a marked reduction in *hGH-N* expression in all six *hGH/P1(ΔHSI)* lines; five of the six *hGH/P1(ΔHSI)* lines expressed *hGH-N* mRNA at levels that were 1%–4% that of the endogenous *mGH* gene and the sixth at 8%. Of note, the expression from the *hGH-N* gene, although markedly reduced secondary to inactivation of HSI, remained site-of-integration independent. The residual *hGH-N* mRNA expression in the *hGH/P1(ΔHSI)* lines also remained pituitary specific (Figure 5B). In contrast to the loss of *hGH-N* expression in the pituitary, the placental expression of the *hCS-A* gene from the *hGH/P1* transgene was unaffected by the HSI deletion. Levels of *hCS-A* mRNA normalized to transgene copy number were equivalent in e18.5 day transgenic placentas of *hGH/P1* and *hGH/P1(ΔHSI)* lines (Figure 5C). Thus, HSI was shown to play a central and tissue-specific role in the remote activation of the *hGH-N* gene in the pituitary. The prior conclusion that specific activation of the pituitary- and placentally expressed genes within the *hGH* locus reflects mechanistically distinct LCR-mediated pathways (Elefant et al., 2000b) was supported by these data as well.

A parallel set of functional studies was applied to a second, unrelated deletion within the *hGH/P1* transgene. A 1.1 kb deletion centered at –28 kb was intro-

duced into the *hGH/P1* transgene by site-specific recombination as was described for HSI (Figure 1B). This deletion removed the region of the LCR encompassing HSIII. Prior cell transfection and transgenic studies had failed to identify a function for HSIII (our unpublished data). The HSIII deletion was introduced into the *hGH/P1* plasmid, and the validated *hGH/P1(ΔHSIII)* plasmid was linearized and used to generate three lines. Pituitary expression of *hGH-N* mRNA in these lines was equivalent to that in lines carrying the intact *hGH/P1* transgene and remained copy number dependent (Figure 5A). These data supported the specific and unique role of HSI in activation of the target *hGH-N* gene.

#### Inactivation of HSI Resulted in Decreased Occupancy of Pit-1 Binding Sites at the *hGH-N* Promoter

Prior studies have established that promoter-proximal Pit-1 binding sites are required for *hGH* gene transcription (Bodner and Karin, 1987; Lefevre et al., 1987). The present study has demonstrated that inactivation of HSI by deletion of a set of Pit-1 sites at –14.5 kb resulted in loss of acetylation at the remote *hGH-N* promoter (Figures 3 and 4) and a corresponding loss of *hGH-N* expression (Figure 5A). To further define the mechanistic link between HSI action and *hGH-N* activation, it was next determined whether occupancy of Pit-1 sites at the *hGH-N* promoter was dependent upon the action of the remote Pit-1 sites at HSI. The levels of Pit-1 occupancy at the *hGH-N* promoter were studied in parallel in two four-copy lines, *hGH/P1* (811D) and *hGH/P1(ΔHSI)* (960G). To facilitate these analyses, the transgenic mice of both lines were crossed with the *hGRF* transgenic line to induce somatotrope hyperplasia. ChIP analyses were carried out on pituitary chromatin from the *hGH/P1* and *hGH/P1(ΔHSI)* lines and from hepatic chromatin from the *hGH/P1* line using an antibody specific to Pit-1 (Figure 6). DNA extracted from input and bound (immunoprecipitated) chromatin fractions were analyzed by quantitative PCR using a set of specific primers that encompassed the promoter-proximal Pit-1 binding sites. Control PCR reactions were carried out using a set of primers specific for the array of functional Pit-1 binding sites in the endogenous murine *thyrotropin*  $\beta$  gene (*TSH $\beta$* ) promoter (Haugen et al., 1996). The immunoprecipitation of pituitary chromatin from the *hGH/P1* mice with the Pit-1 antibody was enriched for *hGH-N* promoter sequences by 28-fold over that in the input chromatin preparation (Figure 6). A parallel ChIP analysis of hepatocyte chromatin from the same mice showed no significant enrichment for *hGH-N* promoter sequences. In contrast to the marked enrichment for *hGH-N* promoter sequences in the pituitary chromatin of the *hGH/P1* line, the same region in the *hGH/P1(ΔHSI)* line was

Figure 4. Inactivation of HSI Resulted in Generalized Loss of Acetylation of Histones H3 and H4 within the *hGH* LCR and at the Remote *hGH-N* Promoter

(A) Acetylation status of histone H3 throughout the *hGH* LCR and *hGH* gene cluster in *hGH/P1* and *hGH/P1(ΔHSI)* transgenic mouse pituitaries. The ChIP assays were carried out as described (Figure 3A) except that only antibody specific for acetylated histone H3 was used. The analysis was carried out in parallel on two *hGH/P1* mouse lines (809F and 811D) and one *hGH/P1(ΔHSI)* transgenic mouse line (960G).

(B) Acetylation status of histone H4 throughout the *hGH* LCR and *hGH* gene cluster in *hGH/P1* and *hGH/P1(ΔHSI)* transgenic mouse pituitaries. The ChIP assays were carried out as described above except that only antibody specific for acetylated histone H4 was used.

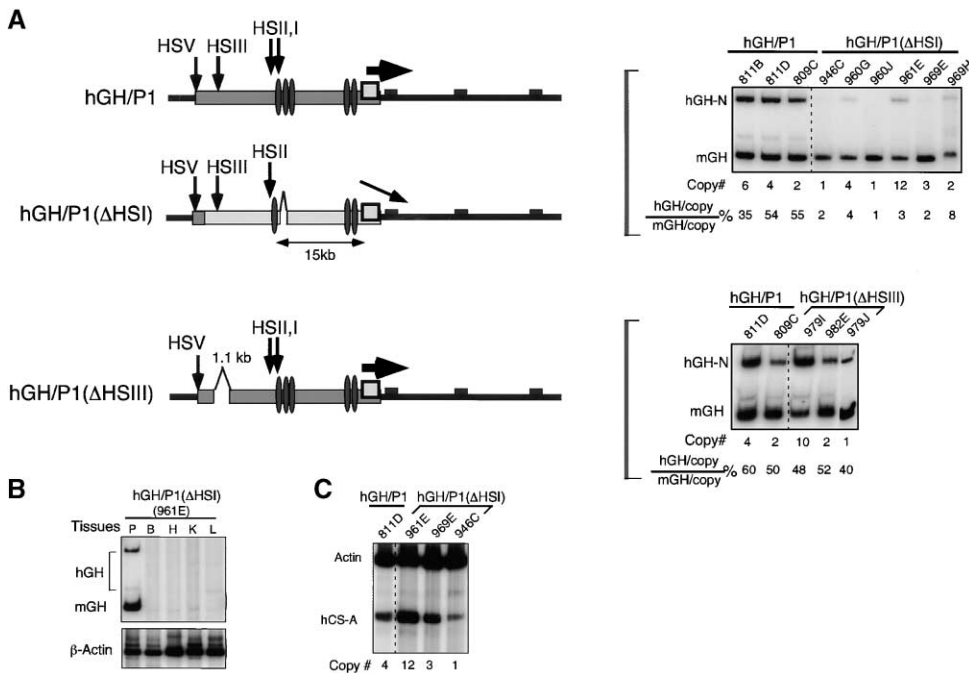


Figure 5. Inactivation of HSI of the *hGH* LCR Resulted in a Marked and Selective Loss of *hGH-N* Expression

(A) Expression of *hGH-N* mRNA in pituitaries of *hGH/P1*, *hGH/P1(ΔHSI)*, and *hGH/P1(ΔHSIII)* mouse lines. The top diagram represents the *hGH/P1* transgene in the pituitary somatotrope. The 32 kb acetylated domain, represented as a shaded rectangle, encompasses the four HS that constitute the *hGH* LCR in pituitary chromatin and extends to include the *hGH-N* promoter. The three Pit-1 binding sites coincident with HSI and the two Pit-1 binding sites within the *hGH-N* gene promoter are indicated (dark ovals). The *hGH-N* gene is depicted (open square) and the bold arrow indicates active transcription. The smaller, solid boxes represent the placental genes in the cluster. The second diagram shows the *hGH/P1(ΔHSI)* transgene. The inactivation of HSI by deletion of the two Pit-1 binding sites is indicated. The loss of acetylation within the LCR and contiguous *hGH-N* promoter is represented by the lighter shading. The selective retention of acetylation at HSV is shown by the darker shading. Loss of *hGH-N* transcription is indicated by the thin, downward-angled arrow. The third diagram shows the *hGH/P1(ΔHSIII)* transgene. Active transcription of *hGH-N* and retention of domain acetylation (not directly documented in this report) are shown. The autoradiographs to the right of the diagrams represent coRT-PCR analyses of the *hGH-N* transgene and endogenous *mGH* expression in pituitaries of the indicated lines. The ratio of pituitary *hGH-N* to *mGH* mRNA in each line was normalized for transgene copy number.

(B) Residual expression of the *hGH-N* mRNA from the *hGH/P1(ΔHSI)* transgene remained pituitary specific. Equal quantities of total RNA from each of the indicated tissues were subjected to coRT-PCR with the primers for *hGH/mGH* and  $\beta$ -actin mRNAs. The signals from full-length and alternatively spliced *hGH* mRNAs are bracketed (P, pituitary; B, brain; H, heart; K, kidney; and L, liver). Ten times more RNA was used per reaction in this study than in (A) to maximize assay sensitivity.

(C) Expression of *hCS-A* mRNA in placentas of *hGH/P1* transgenic embryos was unaffected by HSI inactivation. The autoradiograph contains coRT/PCR analyses of *hCS-A* and  $\beta$ -actin mRNA in placentas of e18.5 day fetuses carrying either the *hGH/P1* or *hGH/P1ΔHSI* transgenes.

only marginally enriched (1.9-fold over input). This marked drop in Pit-1 occupancy in the HSI deletion line was consistent with its very low level of *hGH-N* expression (Figure 5A). Of note, control Pit-1 ChIP study of the endogenous *TSH $\beta$*  promoter revealed equivalent levels of Pit-1 occupancy in the pituitary chromatin of the *hGH/P1* and *hGH/P1(ΔHSI)* lines. These *TSH $\beta$*  promoter ChIP data confirmed the equivalence of the *hGH/P1* and *hGH/P1(ΔHSI)* chromatin preparations. A confirming set of Pit-1 ChIP studies was carried out on additional *hGH/P1* and *hGH/P1(ΔHSI)* lines (809C and 961E), and the marked differential in Pit-1 occupancy was again seen (data not shown). These data indicate that occupancy of the Pit-1 binding sites in the *hGH-N* promoter is dependent on the function of the remote HSI component of the *hGH* LCR.

## Discussion

In previous studies, we showed that an array of Pit-1 binding sites at HSI mediates pituitary-specific and

chromatin-dependent enhancer activity when directly linked to the *hGH-N* gene in a transgenic setting (Benani-Baiti et al., 1998a; Shewchuk et al., 1999). The present study extends these observations by assessing the function of these same HSI determinants when in their native position within the LCR, separated from the target *hGH-N* promoter by 14.5 kb. The data indicate that the HSI determinants play a unique role in activation of the *hGH-N* gene (Figure 5A). The role of the closely linked HSII remains undefined at this point but appears to be minor relative to HSI.

The action of HSI at the level of chromatin structure is supported by the current findings. Deletion of a 99 bp fragment encompassing two active Pit-1 binding sites at HSI resulted in loss of the DNaseI HS site in pituitary chromatin (Figure 2A). More remarkably, this localized deletion resulted in a generalized decrease in acetylation of core histone H3 and H4 throughout the 32 kb pituitary-specific domain that encompasses the *hGH* LCR and linked *hGH-N* promoter (Figures 3 and 4). The effect of HSI on histone acetylation appeared to be

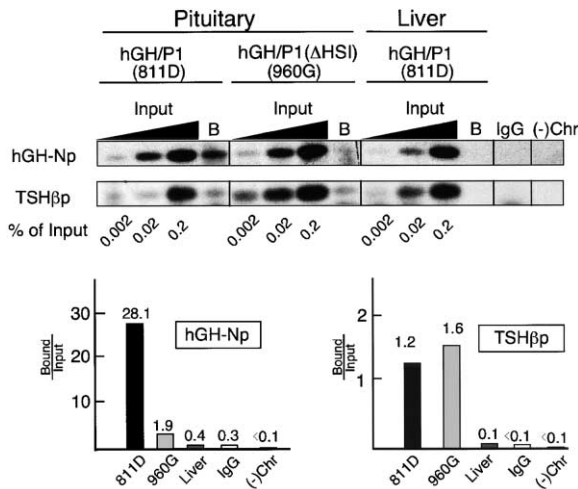


Figure 6. Inactivation of HSI Resulted in a Decrease of Pit-1 Occupancy at the *hGH-N* Promoter-Proximal Binding Sites

Representative Southern blots of Pit-1 ChIP analyses are shown. The DNA isolated from the individual immunoprecipitation reactions was amplified by PCR with primers encompassing the Pit-1 sites in the *hGH-N* and *mTSHβ* promoters. Pituitary and/or hepatic nuclei were isolated from *hGH/P1* and *hGH/P1(ΔHSI)* transgenic mouse lines as indicated. Controls included the use of a nonimmune rabbit antiserum (IgG) and ChIP with no chromatin [(-)Chr]. Signals obtained from bound fractions (B) were normalized to 0.002% of input. The normalized values (bound/input) are plotted on the histogram below.

unique and nonredundant, consistent with its impact on *hGH-N* transcriptional activation. These data constitute an initial *in vivo* demonstration that core histone acetylation of an entire domain can be dependent on a single LCR determinant.

The impact of LCR deletions on chromatin acetylation has been studied previously in a number of model systems. The results of these studies differ in important aspects from the observed global loss of acetylation within the *hGH* LCR subsequent to HSI deletion. For example, deletion of the intensively studied HS2-5 of the human  $\beta$ -globin LCR failed to affect the general pattern of histone H4 acetylation at the  $\beta$ -globin transgene locus. The authors suggested that H4 hyperacetylation at the  $\beta$ -globin locus is independent of the LCR (Schubeler et al., 2000). In a separate report, it was observed that although deletion of the murine  $\beta$ -globin LCR decreased the rate of  $\beta$ -globin transcription, it did not alter the acetylation status of H3 or H4 at the promoters, suggesting that establishment of histone H3 and H4 acetylation at the  $\beta$ -globin gene promoters is independent of LCR function (Schubeler et al., 2001). Analysis of the murine *Igμ* LCR showed that deletion of a defined MAR element significantly reduced histone acetylation at a distal site but had no effect on modification at more proximal intervening sequences (Fernandez et al., 2001). Thus, the linkage of domain-wide acetylation and remote gene activation to HSI function suggests that the *hGH* LCR activates the *hGH-N* promoter via a novel mechanism.

The histone ChIP analyses demonstrated that formation of the 32 kb acetylated chromatin domain encompassing the *hGH* LCR and the contiguous *hGH-N* pro-

moter was uniquely dependent on HSI function (Figures 3 and 4). The levels of acetylation in *hGH/P1(ΔHSI)* were consistently below those seen in the intact *hGH/P1* transgene. The one exception was at HSV where the level of acetylation in two of three lines was comparable to that in the intact LCR when assessed with pooled antibodies. When studied in more detail, it was found that specific H4 acetylation at HSV remained more than 2-fold above genomic background in the HSI deletion line levels (ratio of 2.4), whereas acetylation of H3 was reduced to background level. The selective and focused maintenance of H4 histone acetylation at HSV suggests that an H4-specific HAT coactivator with a spatially limited modifying activity may be independently targeted to this site. Thus, HSV may have a distinct role in LCR function.

Although robust activation of the *hGH-N* promoter was found to be dependent on HSI, the tissue specificity and copy number dependence of *hGH-N* transgene expression appeared to be maintained by other determinants because they were retained in the *hGH/P1(ΔHSI)* transgene. HSV may fulfill this role by insulating the *hGH-N* gene from site-of-integration effects and allowing the *hGH-N* promoter elements to function in a qualitatively normal manner, albeit at very low levels. Such insulator action of HSV is supported by our prior observations that direct juxtaposition of an LCR fragment containing only HSV through HSIII to the *hGH-N* gene with minimal promoter elements resulted in the same low-level, copy number-dependent, and site-of-integration-independence as seen with the *hGH/P1(ΔHSI)* transgene (Figure 5A) (Jones et al., 1995). The present study suggests that HSIII has no significant role in expression of the locus (Figure 5A). In addition, HSV appears to independently recruit coactivators (see above). Thus, a model of *hGH* LCR action consistent with our results would include HSV as a border determinant that serves to insulate the *hGH* locus from outside influences, while HSI would function over substantial distances as a chromatin-dependent transcriptional enhancer.

The specific and nonredundant actions of HSI on core histone acetylation and long-range *hGH-N* gene activation suggest that these two activities are mechanistically linked. This is supported by the specific and essential role played by the 99 bp HSI fragment in domain acetylation and remote *hGH-N* activation (Figures 3, 4, and 5) and by the general relationship between core histone acetylation and gene expression (Pazin and Kadonaga, 1997; Struhl, 1998). A linked action of HSI on histone acetylation and on gene activation is further supported by the observation that Pit-1 interacts with the HAT coactivators CBP/p300 (Xu et al., 1998). On the basis of these data, the initial event in *hGH* LCR function is postulated to be the localized recruitment of HAT coactivators to Pit-1 bound to its cognate sites at HSI. The subsequent extension of the acetylated domain from HSI throughout the LCR, including the contiguous *hGH-N* promoter, would facilitate local access of additional transcriptional activators to their basal promoter binding sites. Interestingly, the basal *hGH-N* promoter itself contains two essential Pit-1 sites (Figure 5A) (Theill et al., 1989) that are dependent on HSI function for full occupancy (Figure 6). This suggests that the Pit-1 sites at HSI and the Pit-1 sites at the target *hGH-N* promoter

have distinct accessibilities within a chromatin context, have distinct functions in gene transactivation, and must be utilized in a defined temporal order. Recent reports of specific allosteric effects of POU-homeodomain binding sites on Pit-1 and Oct-1/Oct-2 functions support a *cis* element-directed mechanism for imparting distinct activities to Pit-1 bound at HSI and at the *hGH-N* promoter (Scully et al., 2000; Tomilin et al., 2000). Defining the basis for the chromatin-dependent, distinct binding specificities for Pit-1 to these two DNA sites is of interest for future studies.

The ChIP experiments using individual antibodies to acetylated H3 or acetylated H4 showed slightly different patterns throughout the *hGH* LCR (Figure 4). Whereas H3 and H4 were both maximally acetylated at the coincident central peak, the pattern of H3 acetylation in the rest of the LCR domain was asymmetric, with higher levels 5' to the peak than at sites between the peak and the *hGH-N* promoter. Histone H4 acetylation was more symmetrically distributed throughout the intact LCR with similar levels at both sides of HSI. These and more subtle differences may reflect interesting diversity in the actions of HAT coactivator complexes and their mechanisms of distribution throughout this region. The biochemical basis underlying the unique role of HSI in establishing the extensive domain of chromatin modification, promoting occupancy at remote *hGH-N* promoter Pit-1 binding sites, as well as long-range activation of *hGH-N* can now be explored in greater detail.

#### Experimental Procedures

##### Deletion of the Pit-1 Binding Sites in the *hGH/P1* Clone

Deletion of the 99 bp fragment (F14.3) containing two Pit-1 binding sites was carried out using a RecA-assisted homologous recombination strategy (Yang et al., 1997) with certain modifications. The deletion was first introduced into a recombination cassette by directly joining 650 bp 5' and 640 bp 3' genomic segments flanking the desired deletion (homology recombination arms A and B; Figure 1A) by splice-overlap extension PCR (SOE-PCR) (Horton et al., 1989) using *Pfu* DNA polymerase. The free 5' and 3' ends of the amplified fragments contained *HindIII* and *Sall* sites, respectively. The recombination cassette was cloned into the pGEM3z vector (Promega) at *HindIII* and *Sall* sites, and the deletion was confirmed by DNA sequencing. The recombination cassette was then transferred to the shuttle vector *pSV1.RecA* (kind gift of N. Heintz, Rockefeller University) (Figure 1B). The resulting plasmid, *pSV1.R-ΔHSI*, was transformed into *E. coli* DH10B carrying the wild-type *hGH/P1* plasmid, and the transformants were grown on Tet- (10 μg/ml) and Kan (25 μg/ml)-containing plates at 30°C overnight. Six to eight colonies were picked and spread on Tet and Kan plates, incubated at 43°C overnight, and the surviving colonies were screened for cointegrants by PCR between primers located 5' of the A arm and within the B arm. Cointegrants were then plated onto Kan LB plates and grown at 43°C overnight to select for the second "resolution" recombination followed by selection on Kan<sup>+</sup> fusaric acid (TB) plates (Yang et al., 1997) at 37°C for 48 hr. Fusaric acid was used to select for Tet-sensitive colonies (Bochner et al., 1980; Maloy and Nunn, 1981). The desired clones were identified by their lack of hybridization to a probe representing the deleted segment. P1 DNA was sequenced across the deletion site to confirm that the recombination occurred at the desired position. A "fingerprinting" approach (Figure 1C) was carried out to confirm that there were no rearrangements or additional deletions anywhere in the *hGH/P1ΔHSI* clone; *hGH/P1* and *hGH/P1ΔHSI* DNAs were digested with *EcoRI* and *BglIII*, electrophoresed through 0.8% agarose gels, transferred to Zetabind nylon membrane (Cuno Inc, Meriden, CT), and hybridized with random primer-labeled *HindIII*-digested *hGH/P1* DNA at 65°C overnight. The

membrane was subsequently washed in 0.1× SSC and 1% SDS at 65°C followed by autoradiography.

##### Generation of Transgenic Mouse Lines

Cesium chloride gradient-purified P1 DNA was linearized with *NotI* (vector site) and purified through an Elutip (Schleicher and Schuell). The DNA was diluted to 2 ng/μl in 10 mM Tris-HCl (pH 7.5) and 0.1 mM EDTA and was microinjected into the pronucleus of C57Bl/6J X SJL mouse zygotes. Founders were identified by dot-blot analysis of tail DNA using as probe a 1.37 kb *SmaI* fragment from *hGH-N* (-494 to +876 relative to the initiation site of *hGH-N* transcription). The integrity of the transgene and its copy number were determined as described (Su et al., 2000).

##### RT-PCR Assays

Pituitary and placental RNAs were prepared from tissues isolated from mice immediately following decapitation and were analyzed by coRT-PCR as previously described (Jones et al., 1995; Su et al., 2000). Briefly, reverse transcription was carried out with 0.5 μg total RNA using 1 U AMV reverse transcriptase (Promega, Madison, WI). Primers used for analysis of *hGH-N* expression corresponded to perfectly conserved regions between *mGH* and *hGH-N*. Following 30 cycles of PCR, the 3' end-labeled products were subjected to *BstNI* digestion at 60°C. The two major bands for *hGH-N* cDNA are 175 bp and 125 bp, corresponding to major and alternative splicing products, respectively (Cooke et al., 1988); the band for *mGH* is 110 bp. Fragments were separated on a 6% polyacrylamide gel, and bands were quantified by phosphorimager analysis (Molecular Dynamics, Sunnyvale, CA). Ratios of *hGH-N* to *mGH* were divided by transgene copy numbers to establish the transgene expression per copy. The primers for *hCS-A* were as previously reported (Su et al., 2000). For the survey of tissue specificity, 5 μg of total RNA from different tissues were used for RT-PCR analysis. A 15 cycle mouse β-actin PCR was used as an internal control.

##### Isolation of Intact Nuclei from the Pituitary

Pituitaries of mice doubly transgenic for the *hGH* cluster and *hGRF* were collected and washed in 20 ml PBS (Ca<sup>2+</sup> and Mg<sup>2+</sup> free). Pituitary cells were dissociated in cell-free dissociation buffer (GIBCO-BRL, Grand Island, NY). Cells were subsequently washed in NB1 buffer (320 mM sucrose, 2 mM MgCl<sub>2</sub>, and 10 mM KPO<sub>4</sub> [pH 6.8]) then in NB2 buffer (10 mM NaCl and 10 mM KPO<sub>4</sub> [pH 6.8]). Cells were lysed in NB3 buffer (320 mM sucrose, 1 mM MgCl<sub>2</sub>, 0.05% Triton X-100, 1 mM PIPES [pH 6.4], and 0.1 mM PMSF). Nuclei were pelleted and suspended in RB buffer (0.1 M NaCl, 50 mM Tris-HCl [pH 8.0], 3 mM MgCl<sub>2</sub>, 0.1 mM PMSF, and 5 mM sodium butyrate [pH 7.0]). The concentration of nuclei was determined by measuring  $A_{260}/A_{280}$ .

##### DNaseI Hypersensitive Site Mapping

300 μg of intact nuclei were suspended in RB with 1 mM CaCl<sub>2</sub> and 100 U DNaseI (GIBCO-BRL). The reaction was incubated at 37°C, and an appropriate volume of reaction (50 μg nuclei) was removed at different time points and added to another tube containing 1/10 volume of 0.5 M EDTA. An equal volume of solution S (1.6 M NaCl, 1% SDS, and 200 μg/ml proteinase K) was added to the tube. The tubes were incubated at 55°C overnight. The samples were phenol/chloroform extracted, EtOH precipitated, and suspended in TE (10 mM Tris, 0.1 mM EDTA). The DNAs were subjected to *EcoRI* digestion, electrophoresis on a 0.8% agarose gel, and then transferred to Zetabind nylon membranes. The membrane was hybridized with 1–2 × 10<sup>6</sup> cpm/ml random primer-labeled probe at 65°C overnight and subsequently washed at 65°C in 0.1× SSC and 1% SDS.

##### Immunoprecipitation of Unfixed Chromatin

Preparation of unfixed chromatin and the chromatin immunoprecipitation (ChIP) assay were carried out as described (Elefant et al., 2000b). Briefly, 0.3 mg nuclei were digested with 25 U of micrococcal nuclease at 37°C for 6 min in 1 ml 50 mM NaCl, 20 mM Tris-HCl (pH 7.5), 3 mM MgCl<sub>2</sub>, 1 mM CaCl<sub>2</sub>, 10 mM sodium butyrate, and 0.1 mM PMSF. The reaction was stopped by the addition of Na<sub>2</sub>EDTA to final concentration of 0.5 mM and salt-soluble chromatin was isolated as described (Hebbes et al., 1994). Soluble chromatin was

concentrated using a Microcentrifugal filter (Amicon Inc., Bedford, PA) and 250  $\mu$ g of this chromatin input was incubated with 10  $\mu$ l each of the antibodies specific against acetylated H3, H4 (Upstate Biotech., Lake Placid, NY), or in the absence of antibody in a total volume of 500  $\mu$ l. Protein A-Sepharose (Amersham Pharmacia Biotech) precipitates were generated and washed, and DNA was purified from the pellets (bound) and supernatants (unbound) as described (O'Neill and Turner, 1996). DNA samples from the input, bound, and unbound fractions were analyzed by electrophoresis on 1% agarose gels to determine the size distribution of the resulting oligonucleosomes. 1  $\mu$ g of DNA from each of the fractions was loaded onto Zetabind nylon membranes using a slot-blot manifold. The blots were hybridized with  $1-2 \times 10^6$  cpm/ml random primer-labeled probe at 65°C overnight. The membrane was subsequently washed at 60°C in 0.1% SDS and  $0.5 \times$  SSC. Signals were quantified by phosphorimager analysis. The ratios between bound and unbound DNA fractions were calculated for each probe used. All ratios were normalized for DNA loading by rehybridizing the membrane with [ $^{32}$ P]-labeled total mouse genomic DNA (Elefant et al., 2000a).

#### Immunoprecipitation of Fixed Chromatin

ChIP with antibody against Pit-1 was performed as described (Forsberg et al., 2000) with minor modifications. Single-cell suspensions from pituitaries of mice doubly transgenic for the *hGH* cluster and *hGRF* were transferred to 50 ml DMEM and 10% FBS. The cell suspensions were fixed in 1% formaldehyde at RT for 10 min followed by the addition of glycine (0.125 M) with incubation at room temperature (RT) for an additional 5 min. Cells were collected, washed twice with cold PBS twice, and lysed in NB3 buffer. Pelleted nuclei were suspended in lysis buffer (50 mM Tris-HCl [pH 8.1], 10 mM EDTA, 1% SDS, 10 mM sodium butyrate, and 0.1 mM PMSF) and incubated on ice for 10 min. The lysates were then sheared (Sonic Dismembrator, Fisher Scientific) to an average size of 1 kb, and the soluble chromatin was concentrated using Centricon-10 (Amicon Inc., Bedford, PA) and taken up in IP buffer (20 mM Tris-HCl [pH 8.1], 150 mM NaCl, 2 mM EDTA, 0.01% SDS, 1% Triton X-100, 10 mM sodium butyrate, and 0.1 mM PMSF). An aliquot of each sample was removed as "input" and used in PCR analysis. The remainder of the soluble chromatin was incubated at 4°C overnight with 20  $\mu$ l of Pit-1 antibody (Santa Cruz Biotechnology, Inc, Santa Cruz, CA) or preimmune IgG (Upstate Biotech, Lake Placid, NY). Immune complexes were isolated by incubation with 60  $\mu$ l of Protein A-agarose for 2 hr at 4°C. The complexes were serially washed in 1 ml low salt buffer (0.1% SDS, 1% Triton X-100, 2 mM EDTA, 20 mM Tris-HCl [pH 8.1], and 150 mM NaCl), 1 ml of the same buffer but with high salt (500 mM NaCl), 1 ml of LiCl buffer (250 mM LiCl, 1% NP-40, 1% sodium deoxycholate, 1 mM EDTA, and 10 mM Tris-HCl [pH 8.1]), and twice with TE (10 mM Tris-HCl [pH 8.0] and 1 mM EDTA). The complexes were eluted with two 250  $\mu$ l aliquots of elution buffer (1% SDS and 0.1 M NaHCO<sub>3</sub>) at RT for 15 min. DNA was isolated by reversing the cross-links; samples were heated at 65°C for 5 hr in the presence of 0.2 M NaCl and 2  $\mu$ l of 10 mg/ml RNase A and subsequently digested with 1  $\mu$ l of 20 mg/ml proteinase K at 45°C for 12 hr. The purified DNA was resuspended in 40  $\mu$ l of water and analyzed by PCR with specified primer pairs. PCR products were resolved on 2% agarose gels, transferred to Zetabind nylon membranes, and hybridized with  $^{32}$ P-labeled probe at 42°C for 2 hr. The membrane was subsequently washed at 42°C in 0.1% SDS and  $0.5 \times$  SSC, and signals were quantified by phosphorimager analysis. Band intensities were expressed relative to the signal obtained from 0.002% of input, and all signals were demonstrated to be proportional to the amount of DNA input.

#### Primer and Probe Preparation

Primers for recombination arms were: arm A (5' arm), 5'-AGG AAGCTTGTCCACCAGTGAGGGAACAGAC-3' and 5'-GTTCTTTCTCA GCTTGAGGCCCATGGGCC-3'; arm B (3' arm), 5'-ACGCGTCGA CTTCTGGGCAGGGAACAGGAGCT-3' and 5'-CTCAAGCTGAGAA AGAACATCTGGGGCTGC-3'.

The series of unique sequence probes for chromatin immunoprecipitation slot blot assays were generated by PCR using AmpliTaq DNA polymerase (Perkin-Elmer). The *hGH/P1* clone was used as the PCR template. The primer sets were as described (Elefant et al.,

2000a, 2000b). Probes for DNase I HS mapping were generated by PCR using the following primer sets—the HSI,II probe: 5' primer, 5'-ACAGGCTGCAGCCGGTGCAGTT-3' and 3' primer, 5'-CCCTC CTGCAGGACTGGGTCC-3'; the HSIII-V probe: 5' primer, 5'-CTAG GGAATTCCTGAGCTGGCC-3' and 3' primer, 5'-GGAGAACCCGGG CACCAGTGT-3'; the primer set for amplification of the *hGH-N* promoter was 5' primer, 5'-CAGGGCTATGGGAGGAAGAGCTT-3' and 3' primer, 5'-CTTCTCCCCTGTTGCC-3'; and the primer set for amplification of TSH $\beta$  promoter was 5' primer, 5'-GTTTCAGGGG GAGGATATAGTG-3' and 3' primer, 5'-ATCTTACAGGTTCTGCA CAGGG-3'.

#### Acknowledgments

This research was supported by a grant from the National Institutes of Health (HD25147) to N.E.C and S.A.L., by National Research Service Awards to Y.H. (F32-DK-10051) and F.E. (F32-HD-08471), and in part from support from the Howard Hughes Medical Institute. We are grateful to the Transgenic and Chimeric Mouse Core of the University of Pennsylvania for generation of all transgenic lines.

Received August 3, 2001; revised November 30, 2001.

#### References

- Bennani-Baiti, I.M., Jones, B.K., Liebhauer, S.A., and Cooke, N.E. (1995). Physical linkage of the human growth hormone gene cluster and the skeletal muscle sodium channel alpha-subunit gene (*SCN4A*) on chromosome 17. *Genomics* 29, 647–652.
- Bennani-Baiti, I.M., Asa, S.L., Song, D., Iratni, R., Liebhauer, S.A., and Cooke, N.E. (1998a). DNase I-hypersensitive sites I and II of the human growth hormone locus control region are a major developmental activator of somatotrope gene expression. *Proc. Natl. Acad. Sci. USA* 95, 10655–10660.
- Bennani-Baiti, I.M., Cooke, N.E., and Liebhauer, S.A. (1998b). Physical linkage of the human growth hormone gene cluster and the *CD79b* (*Ig  $\beta$ /B29*) gene. *Genomics* 48, 258–264.
- Bochner, B.R., Huang, H.C., Schieven, G.L., and Ames, B.N. (1980). Positive selection for loss of tetracycline resistance. *J. Bacteriol.* 143, 926–933.
- Bodner, M., and Karin, M. (1987). A pituitary-specific *trans*-acting factor can stimulate transcription from the growth hormone promoter in extracts of nonexpressing cells. *Cell* 50, 267–275.
- Chen, E.Y., Liao, Y.C., Smith, D.H., Barrera-Saldana, H.A., Gelinis, R.E., and Seeburg, P.H. (1989). The human growth hormone locus: nucleotide sequence, biology, and evolution. *Genomics* 4, 479–497.
- Cooke, N.E., and Liebhauer, S.A. (1995). Molecular biology of the growth hormone-prolactin gene system. *Vitam. Horm.* 50, 385–459.
- Cooke, N.E., Ray, J., Watson, M.A., Estes, P.A., Kuo, B.A., and Liebhauer, S.A. (1988). Human growth hormone gene and the highly homologous growth hormone variant gene display different splicing patterns. *J. Clin. Invest.* 82, 270–275.
- Elefant, F., Cooke, N.E., and Liebhauer, S.A. (2000a). Targeted recruitment of histone acetyltransferase activity to a locus control region. *J. Biol. Chem.* 275, 13827–13834.
- Elefant, F., Su, Y., Liebhauer, S.A., and Cooke, N.E. (2000b). Patterns of histone acetylation suggest dual pathways for gene activation by a bifunctional locus control region. *EMBO J.* 19, 6814–6822.
- Felsenfeld, G., Boyes, J., Chung, J., Clark, D., and Studitsky, V. (1996). Chromatin structure and gene expression. *Proc. Natl. Acad. Sci. USA* 93, 9384–9388.
- Fernandez, L.A., Winkler, M., and Grosschedl, R. (2001). Matrix attachment region-dependent function of the immunoglobulin  $\mu$  enhancer involves histone acetylation at a distance without changes in enhancer occupancy. *Mol. Cell. Biol.* 21, 196–208.
- Festenstein, R., Tolaini, M., Corbella, P., Mamalaki, C., Parrington, J., Fox, M., Miliou, A., Jones, M., and Kioussis, D. (1996). Locus control region function and heterochromatin-induced position effect variegation. *Science* 271, 1123–1125.
- Forsberg, E.C., Downs, K.M., Christensen, H.M., Im, H., Nuzzi, P.A.,

- and Bresnick, E.H. (2000). Developmentally dynamic histone acetylation pattern of a tissue-specific chromatin domain. *Proc. Natl. Acad. Sci. USA* 97, 14494–14499.
- Grosveld, F., van Assendelft, G.B., Greaves, D.R., and Kollias, G. (1987). Position-independent, high-level expression of the human  $\beta$ -globin gene in transgenic mice. *Cell* 51, 975–985.
- Grunstein, M. (1997). Histone acetylation in chromatin structure and transcription. *Nature* 389, 349–352.
- Hamilton, C.M., Aldea, M., Washburn, B.K., Babitzke, P., and Kushner, S.R. (1989). New method for generating deletions and gene replacements in *Escherichia coli*. *J. Bacteriol.* 171, 4617–4622.
- Haugen, B.R., McDermott, M.T., Gordon, D.F., Rupp, C.L., Wood, W.M., and Ridgway, E.C. (1996). Determinants of thyrotrope-specific thyrotropin  $\beta$  promoter activation. Cooperation of Pit-1 with another factor. *J. Biol. Chem.* 271, 385–389.
- Hebbes, T.R., Clayton, A.L., Thorne, A.W., and Crane-Robinson, C. (1994). Core histone hyperacetylation co-maps with generalized DNase I sensitivity in the chicken  $\beta$ -globin chromosomal domain. *EMBO J.* 13, 1823–1830.
- Horton, R.M., Hunt, H.D., Ho, S.N., Pullen, J.K., and Pease, L.R. (1989). Engineering hybrid genes without the use of restriction enzymes: gene splicing by overlap extension. *Gene* 77, 61–68.
- Jones, B.K., Monks, B.R., Liebhaber, S.A., and Cooke, N.E. (1995). The human growth hormone gene is regulated by a multicomponent locus control region. *Mol. Cell. Biol.* 15, 7010–7021.
- Kuo, M.H., and Allis, C.D. (1998). Roles of histone acetyltransferases and deacetylases in gene regulation. *Bioessays* 20, 615–626.
- Lefevre, C., Imagawa, M., Dana, S., Grindlay, J., Bodner, M., and Karin, M. (1987). Tissue-specific expression of the human growth hormone gene is conferred in part by the binding of a specific trans-acting factor. *EMBO J.* 6, 971–981.
- Lewis. (1992). Growth hormone: what is it and what does it do? *Trends Endocrinol. Metab.* 3, 117–121.
- Li, Q., Harju, S., and Peterson, K.R. (1999). Locus control regions: coming of age at a decade plus. *Trends Genet.* 15, 403–408.
- Maloy, S.R., and Nunn, W.D. (1981). Selection for loss of tetracycline resistance by *Escherichia coli*. *J. Bacteriol.* 145, 1110–1111.
- Mayo, K.E., Hammer, R.E., Swanson, L.W., Brinster, R.L., Rosenfeld, M.G., and Evans, R.M. (1988). Dramatic pituitary hyperplasia in transgenic mice expressing a human growth hormone-releasing factor gene. *Mol. Endocrinol.* 2, 606–612.
- O'Connor, M., Peifer, M., and Bender, W. (1989). Construction of large DNA segments in *Escherichia coli*. *Science* 244, 1307–1312.
- O'Neill, L.P., and Turner, B.M. (1996). Immunoprecipitation of chromatin. *Methods Enzymol.* 274, 189–197.
- Pazin, M.J., and Kadonaga, J.T. (1997). What's up and down with histone deacetylation and transcription? *Cell* 89, 325–328.
- Schubeler, D., Francastel, C., Cimborra, D.M., Reik, A., Martin, D.I., and Groudine, M. (2000). Nuclear localization and histone acetylation: a pathway for chromatin opening and transcriptional activation of the human  $\beta$ -globin locus. *Genes Dev.* 14, 940–950.
- Schubeler, D., Groudine, M., and Bender, M.A. (2001). The murine  $\beta$ -globin locus control region regulates the rate of transcription but not the hyperacetylation of histones at the active genes. *Proc. Natl. Acad. Sci. USA* 98, 11432–11437.
- Scully, K.M., Jacobson, E.M., Jepsen, K., Lunyak, V., Viadiu, H., Carriere, C., Rose, D.W., Hooshmand, F., Aggarwal, A.K., and Rosenfeld, M.G. (2000). Allosteric effects of Pit-1 DNA sites on long-term repression in cell type specification. *Science* 290, 1127–1131.
- Shashikant, C.S., Carr, J.L., Bhargava, J., Bentley, K.L., and Ruddle, F.H. (1998). Recombinogenic targeting: a new approach to genomic analysis—a review. *Gene* 223, 9–20.
- Shewchuk, B.M., Asa, S.L., Cooke, N.E., and Liebhaber, S.A. (1999). Pit-1 binding sites at the somatotrope-specific DNase I hypersensitive sites I, II of the human growth hormone locus control region are essential for in vivo hGH-N gene activation. *J. Biol. Chem.* 274, 35725–35733.
- Struhl, K. (1998). Histone acetylation and transcriptional regulatory mechanisms. *Genes Dev.* 12, 599–606.
- Su, Y., Liebhaber, S.A., and Cooke, N.E. (2000). The human growth hormone gene cluster locus control region supports position-independent pituitary- and placenta-specific expression in the transgenic mouse. *J. Biol. Chem.* 275, 7902–7909.
- Theill, L.E., Castrillo, J.L., Wu, D., and Karin, M. (1989). Dissection of functional domains of the pituitary-specific transcription factor GHF-1. *Nature* 342, 945–948.
- Tomilin, A., Remenyi, A., Lins, K., Bak, H., Leidel, S., Vriend, G., Wilmanns, M., and Scholer, H.R. (2000). Synergism with the coactivator OBF-1 (OCA-B, BOB-1) is mediated by a specific POU dimer configuration. *Cell* 103, 853–864.
- Xu, L., Lavinsky, R.M., Dasen, J.S., Flynn, S.E., McInerney, E.M., Mullen, T.M., Heinzel, T., Szeto, D., Korzus, E., Kurokawa, R., et al. (1998). Signal-specific co-activator domain requirements for Pit-1 activation. *Nature* 395, 301–306.
- Yang, X.W., Model, P., and Heintz, N. (1997). Homologous recombination based modification in *Escherichia coli* and germline transmission in transgenic mice of a bacterial artificial chromosome. *Nat. Biotechnol.* 15, 859–865.
- Zhang, Y., Buchholz, F., Muyrers, J.P., and Stewart, A.F. (1998). A new logic for DNA engineering using recombination in *Escherichia coli*. *Nat. Genet.* 20, 123–128.